ELSEVIER

Contents lists available at ScienceDirect

Science Bulletin

journal homepage: www.elsevier.com/locate/scib



Article

High-temperature treatment induced carbon anode with ultrahigh Na storage capacity at low-voltage plateau

Chenglong Zhao a,b, Qidi Wang c,d, Yaxiang Lu a,b,*, Baohua Li c, Liquan Chen a,b, Yong-Sheng Hu a,b,*

- ^a Key Laboratory for Renewable Energy, Beijing Key Laboratory for New Energy Materials and Devices, Beijing National Laboratory for Condensed Matter Physics, Institute of Physics, Chinese Academy of Sciences, Beijing 100190, China
- ^b School of Physical Sciences, University of Chinese Academy of Sciences, Beijing 100049, China
- ^c Division of Energy and Environment, Engineering Laboratory for the Next Generation Power and Energy Storage Batteries, Graduate School at Shenzhen, Tsinghua University, Shenzhen, 518055. China
- ^d School of Materials Science and Engineering, Tsinghua University, Beijing 100084, China

ARTICLE INFO

Article history: Received 23 July 2018 Received in revised form 23 July 2018 Accepted 23 July 2018 Available online 25 July 2018

Keywords:
Sodium-ion battery
Na storage
Hard carbon
Charcoal
High-temperature carbonization
Low-voltage plateau

ABSTRACT

Sodium-ion batteries (NIBs) show great prospect on the energy storage applications benefiting from their low cost and the abundant Na resources despite the expected lower energy density compared with lithium-ion batteries (LIBs). To further enhance the competitive advantage, especially in energy density, developing the high-capacity carbon anode materials can be one of the effective approaches to realize this goal. Herein, we report a novel carbon anode made from charcoal with a high capacity of \sim 400 m Ah g⁻¹, wherein about 85% (>330 mAh g⁻¹) of its total capacity is derived from the long plateau region below \sim 0.1 V, which differs from those of typical hard carbon materials (\sim 300 mAh g⁻¹) in NIBs but is similar to the graphite anode in LIBs. When coupled with air-stable Na_{0.9}Cu_{0.22}Fe_{0.30}Mn_{0.48}O₂ oxide cathode, a high-energy density of \sim 240 Wh kg⁻¹ is achieved with good rate capability and cycling stability. The discovery of this promising carbon anode is expected to further improve the energy density of NIBs towards large-scale electrical energy storage.

© 2018 Science China Press. Published by Elsevier B.V. and Science China Press. All rights reserved.

1. Introduction

Lithium-ion batteries (LIBs) show the highest energy density in commercial rechargeable batteries and have been widely applied in consumer electronics and electric vehicles (EVs). To meet the increasing requirement of large-scale electrical energy storage applications, LIBs may not be the rational choice due to the limited lithium and cobalt resources in the future [1-3]. Since 2010, sodium-ion batteries (NIBs) have been intensively investigated as one of the promising alternatives to LIBs in terms of the gridscale energy storage because of their low cost and resource advantages. However, the energy density of the current NIBs remains a challenge hindering its large-scale commercial application [4–8]. Developing the high-capacity electrode materials including cathode and anode materials is the primary solution at moment. Recently, several cathode materials such as layered oxides $(Na_{0.9}Cu_{0.22}Fe_{0.30}Mn_{0.48}O_2, \quad NaNi_{0.33}Fe_{0.33}Mn_{0.33}O_2, \quad etc.) \quad \ [9-11],$ Prussian blue compounds (Na_xFe₂(CN)₆, etc.) [12], polyanionic compounds (Na₃V₂(PO₄)₂F₃, etc.) [13] have been explored to be fabricated in NIBs due to the high-energy density and easy synthesis process. Regarding to anodes, hard carbon is one of the most promising materials for the early NIBs due to their good comprehensive performance, e.g., high capacity (~300 mAh g⁻¹), good cycling stability, high initial Coulombic efficiency, and abundant precursor resources [8,14]. Further increasing the energy density largely relies on the improvement of electrode materials. However, limited by the fixed crystal structure framework, molecular weight and redox potential, cathode materials are very difficult to make every step forward. Instead, carbon anodes have plenty of room to be improved due to the flexible tuning parameters including precursor choice, heteroatom doping, carbonization temperature control, keeping time, pretreatment process (acid/alkali washing, pore-forming agent addition, pyrolysis atmosphere, microwave treatment), etc., which greatly influence the microstructure of prepared carbon materials [14–24].

The structure-property relationship is a good guidance to design novel carbon anodes. Until now, most NIB carbon anodes with high performance normally demonstrate consistent behaviour in the discharge-charge curve with two distinct regions: a slope region above $\sim\!0.1$ V and plateau region below $\sim\!0.1$ V. Usually, the plateau region exhibits a higher capacity (<220 mAh g $^{-1}$) than that of the slope region, which contributes more to the total capacity. In addition, the low-potential plateau can further

^{*} Corresponding authors.

E-mail addresses: yxlu@iphy.ac.cn (Y. Lu), yshu@iphy.ac.cn (Y.-S. Hu).

increase the energy density of full cells to some extent. Therefore, designing and discovering a carbon anode with a large proportion of the plateau capacity can be a potential approach to increase the energy density of NIBs [14].

Here we have conducted a lot of experimental designs to regulate an effective microstructure to increase the ratio of plateau capacity involved all the strategies above-mentioned. Fortunately, we discovered a carbon anode made from charcoal with about 85% (>330 mAh g $^{-1}$) of total capacity contributed to a long low-voltage plateau below $\sim\!0.1$ V, realizing a high-capacity anode $\sim\!400$ mAh g $^{-1}$ for NIBs. The as-prepared carbon anode exhibits a honeycomb-like microstructure with large internal pores linked with graphitic layers, which is different from the commonly turbostratic nanodomains. Furthermore, full cells coupled the resulting anode with layered Na $_{0.9}$ Cu $_{0.22}$ Fe $_{0.30}$ Mn $_{0.48}$ O $_{2}$ oxide cathode show the highenergy density of $\sim\!240$ Wh kg $^{-1}$ with stable cycling performance. This carbon anode with large proportion of the plateau capacity has not been reported in NIBs so far, and its emergence may open up a new avenue towards the high-energy density NIBs.

2. Experimental

2.1. Sample preparation

Charcoal derived from wood was used as precursor material to prepare the desired carbon anode. Firstly, the sample was heated at 800 °C for 3 h with a heating rate of 10 °C min⁻¹ in a tube furnace under argon flow; after cooling to room temperature a series of repeated washing with dilute hydrochloric acid (30%) and deionized water was carried out. Then the grinded samples were dried at 120 °C under vacuum for 12 h. Secondly, the obtained materials were carbonized at a high-temperature graphite furnace under argon flow at 1,900 °C for 3 h with a heating rate of 3 °C min⁻¹. The above-mentioned washing, grinding and drying processes should be repeated after this step. Then, the material was directly put into an Ar-filled glovebox to prevent any moisture exposition. The cathode material was prepared by a solid-state reaction using precursors of Na₂CO₃ (99.5%), CuO (98%), Fe₂O₃ (99%) and Mn₂O₃ (98%). The starting materials were ball-milled on the PM 100 equipment at 400 r min⁻¹ for 10 h and pressed into pellets under pressure of 8 MPa. Then the pellets were heated at 900 °C for 12 h in air.

2.2. Materials characterizations

Powder X-ray diffraction (XRD) was performed using a Bruker D8 Advance diffractometer equipped with a Cu K α radiation source (λ_1 = 1.54060 Å, λ_2 = 1.54439 Å) and a LynxEye_XE detector. The morphologies of the materials were investigated using a scanning electron microscope (Hitachi S-4800) in combination with energy dispersive X-ray spectroscopy (EDS). High-resolution transmission electron microscopy (HR-TEM) images and the corresponding selected area electron diffraction (SAED) patterns were characterized by transmission electron microscopy (TEM) (JEM 2100F) with an accelerating voltage of 200 kV. The Raman spectra were recorded using a Horiva (JY-HR800 micro-Raman) spectrometer. Nitrogen adsorption/desorption isotherms were tested on ASAP2020M+C at 77 K and the specific surface area and pore diameter distribution were calculated by Brunauer-Emmett-Teller method (BET) and Barrett-Joyner-Halenda method (BJH), respectively.

2.3. Electrochemical measurement.

The working electrodes were prepared via mixing 80 wt% active material with 10 wt% conductive additives (acetylene black: super

P = 8:2) and 10 wt% sodium alginate binder on Cu foil with the loading mass of the active material was \sim 2 mg cm⁻². The prepared electrodes were dried at 120 °C under vacuum for 10 h and then were fabricated into CR2032 coin-type cells with pure sodium foil as the counter electrode in an argon-filled glove box (H_2O , $O_2 < 0.1$ ppm). A glass fiber was used as the separator, and the electrolyte was a solution of 1 mol L^{-1} NaPF₆ in ethylene (EC) and dimethyl carbonate (DMC) (1:1 in volume) with 5% fluoroethylene carbonate (FEC) in volume. All the operations were performed in the Argon-filled glove box. The discharge and charge tests were carried out on a Land BT2000 battery test system (Wuhan, China). Cycling voltammetry measurements were carried out at a scan rate of 0.1 mV s⁻¹ using an Autolab PG302N electrochemical workstation. Na-ion full cells were constructed using the as-prepared carbon anode material and layered Na_{0.9}Cu_{0.22}Fe_{0.30}Mn_{0.48}O₂ as the cathode material in a CR2032 coin-type cell. The weight ratio of the two electrodes (anode/cathode) was ~1:4.08. The full cells were charged and discharged in a voltage range of 1-4.05 V.

3. Results and discussion

Microstructures of this as-prepared carbon anode were investigated by XRD and Raman spectra analysis shown in Fig. 1a and b. The Bragg diffractions exhibit the broad peaks at around 24.3° and 43.1° corresponding to the diffraction of (0 0 2) and (1 0 0) planes in the disordered amorphous structure, while a sharp peak at 25.5° was also found indexed in the (0 0 2) plane of ordered graphitized structure. Raman spectrum shows two separate typical bands: the defect-induced peak at 1,343 cm $^{-1}$ (D-band) and the crystalline graphite band at 1,588 cm $^{-1}$ (G-band peak), where the integrate intensity ratio of G-band and D-band can be used to reflect the defects concentration along the graphitic layers with the value of $I_{\rm D}/I_{\rm G}\sim 1.45$ further confirmed the amorphous characteristics. What is worth noting that the 2D, D+G and 2D′ bands,

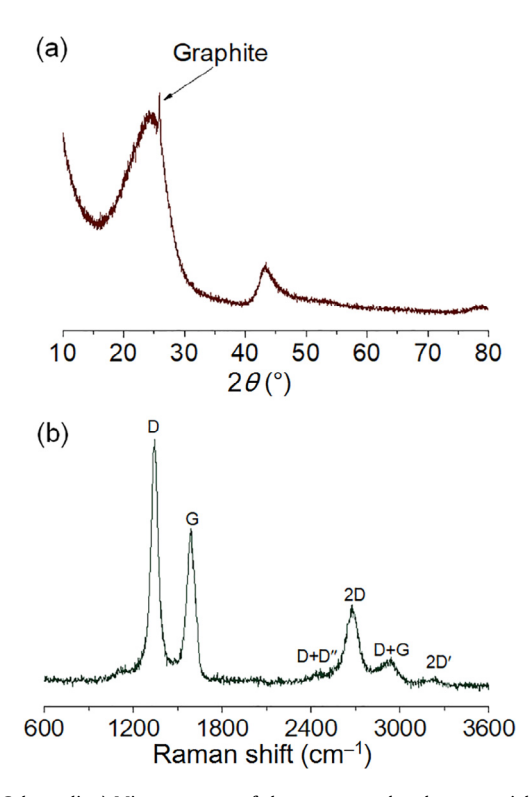
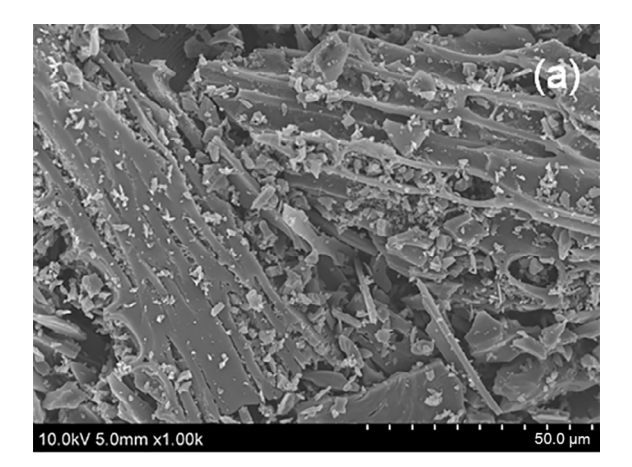


Fig. 1. (Color online) Microstructure of the as-prepared carbon material. (a) XRD pattern of the as-prepared sample indexed with amorphous and graphitized peaks. (b) Raman spectrum of D, G, D + D", 2D, D + G and 2D' bands.

which are typical graphite bands for the highly ordered carbon material, are also observed. Both the XRD pattern and Raman spectrum demonstrate the mixed amorphous and graphitized structures.

Furthermore, the microstructures were observed by SEM and TEM as shown in Fig. 2a and b. The SEM image of the asprepared sample shows a honeycomb-like structure after carbonized at high temperature, exhibiting the natural pores and channels with a well-connection architecture. Meanwhile, TEM image also shows a honeycomb-like microstructure with large internal pores linked with graphitic layers, which is different from the commonly crosslinked turbostratic nanodomains and pores of the hard carbon anodes. And the sharpness of the dispersed diffraction rings of the SAED pattern implies the gradual development of the graphitic local structure. Given that the charcoal is a hard carbon precursor which cannot be fully graphitized at a high temperature of 1.900 °C, the partial graphitization at a limited scale to form a mixture of order and disorder texture could be realized instead. The so-called bi-honeycomb-like architecture of this carbon material not only facilitates the Na⁺ ion storage but also improves electrolyte infiltration to promote Na⁺ ion transfer and diffusion. Interestingly, the Brunauer-Emmett-Teller (BET) surface area of this sample measured by the N2 adsorption-desorption was quite small and is only 1.48 m 2 g $^{-1}$; and this low surface area could induce limited solid electrolyte interphase (SEI) formation leading to a high initial Coulombic efficiency.

To evaluate the electrochemical properties, half cells with Na metal as a counter electrode and full cells with layered Na $_{0.9}$ Cu $_{0.22}$ Fe $_{0.30}$ Mn $_{0.48}$ O $_2$ oxide as a cathode are fabricated and tested. Fig. 3a shows the galvanostatic discharge-charge profiles of the carbon anode in a voltage range of 0–2.5 V vs. Na $^+$ /Na at a current density of \sim 25 mA g $^{-1}$ (0.05C). Surprisingly, this carbon anode shows a large proportion of the plateau capacity about 85% (>330 mAh g $^{-1}$) of total reversible capacity of \sim 400 mAh g $^{-1}$ at



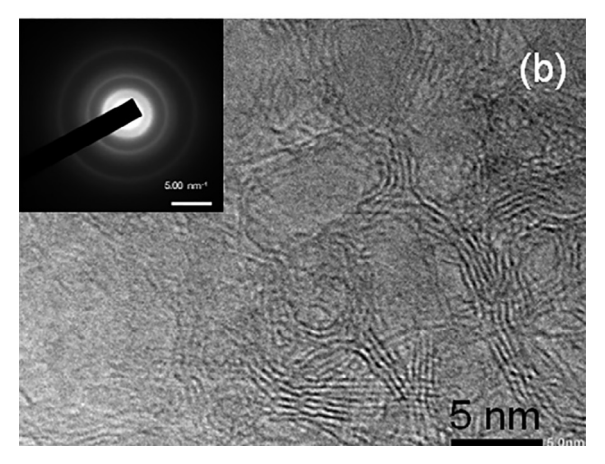


Fig. 2. Observation of the as-prepared carbon material. (a) SEM and (b) TEM images showing the honeycomb-like structure of the obtained carbon anode material.

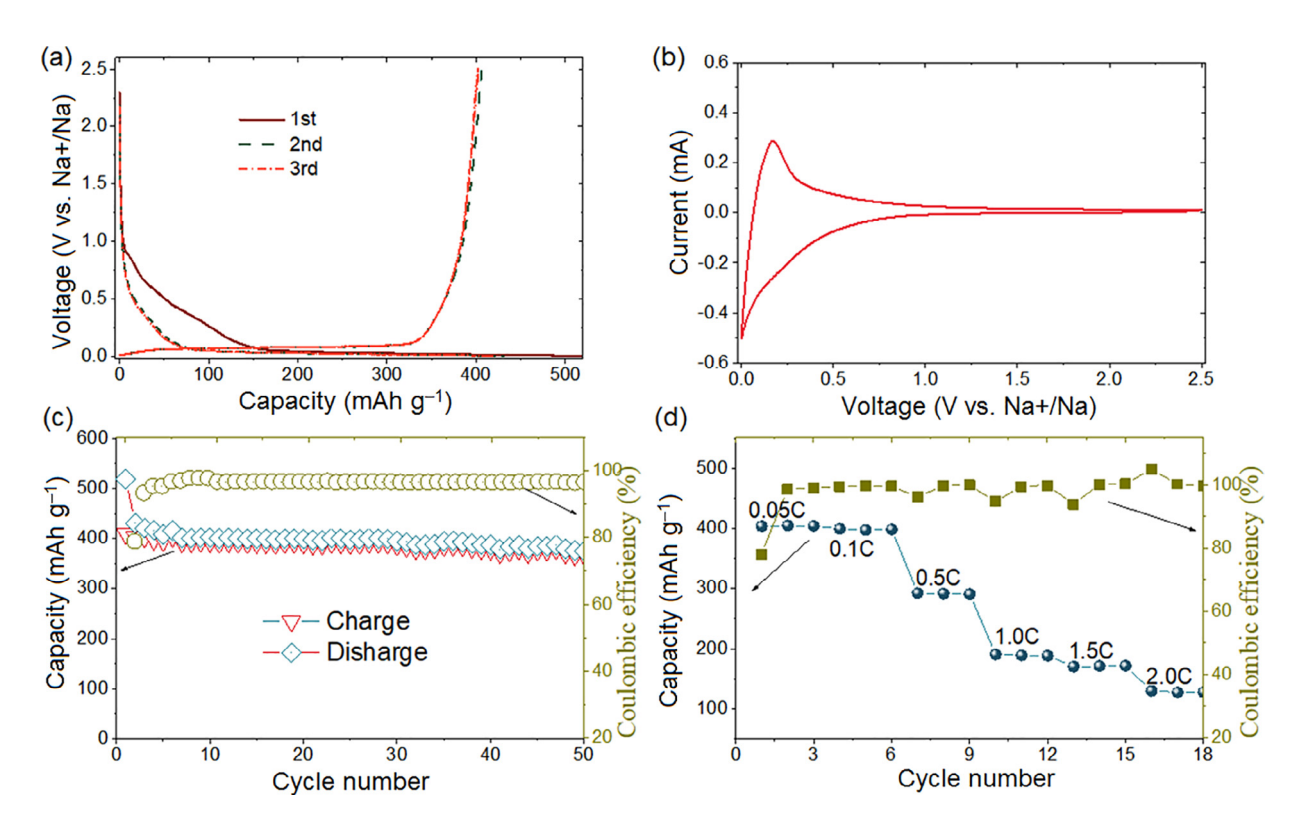
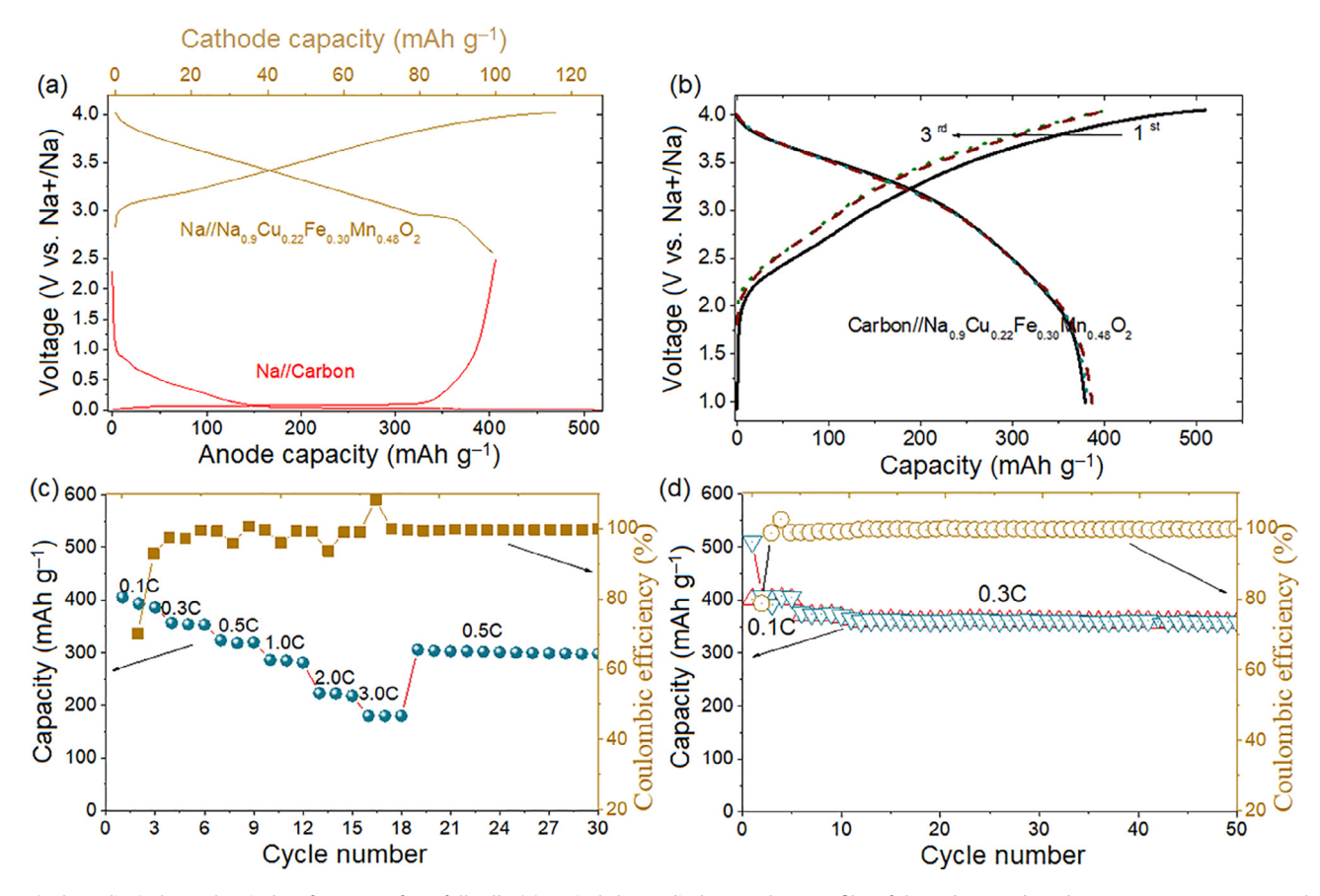


Fig. 3. (Color online) Electrochemical properties of the carbon anode in half cells. (a) Galvanostatic discharge-charge curves, (b) CV curves, (c) cycling performance and (d) rate capability.



 $\textbf{Fig. 4.} \ \ (\text{Color online}) \ \ \text{Electrochemical performance of NIB full cells. (a) Typical charge-discharge voltage profiles of the carbon anode and $Na_{0.9}Cu_{0.22}Fe_{0.30}Mn_{0.48}O_2$ cathode, respectively. Electrochemical performance of the carbon//Na_{0.9}Cu_{0.22}Fe_{0.30}Mn_{0.48}O_2$ full cell, (b) charge-discharge curves, (c) rate capability and (d) cycling performance.$

the low potential below ~ 0.1 V. A high initial Coulombic efficiency of 80% was found for this anode related to its optimized microstructure and less formation of SEI. CV measurement in Fig. 3b shows a pair of redox peaks at ~ 0.1 V similar to other hard carbon anodes. The reversible peaks also indicate the less formation of SEI and a higher initial Coulombic efficiency. Cycling stability and rate capability are tested and shown in Fig. 3c and d. After 50 cycles at a current rate of 0.1C, the capacity retention is 91.5%, which suggests a good stability of this high-capacity anode. In addition, it exhibits a good rate performance with specific capacities of 294, 192 and 124 mAh g $^{-1}$ at current rates of 0.5C, 1C and 2C, respectively.

In order to demonstrate the actual performance of this anode, the coin-type NIB full cells with the as-prepared carbon anode and layered $Na_{0.9}Cu_{0.22}Fe_{0.30}Mn_{0.48}O_2$ oxide cathode were fabricated and the electrochemical performance is shown in Fig. 4. Fig. 4a illustrates the charge-discharge voltage profiles of the carbon anode and Na_{0.9}Cu_{0.22}Fe_{0.30}Mn_{0.48}O₂ cathode at 0.1C rate. The typical charge-discharge profiles of carbon// Na_{0.9}Cu_{0.22}Fe_{0.30}Mn_{0.48}O₂ full cells are shown in Fig. 4b at a current rate of 0.1C in the voltage range of 1-4.05 V, which delivers a high reversible capacity of ~390 mAh g⁻¹ based on the mass of the carbon anode with the initial Coulombic efficiency of \sim 76% and the average operation voltage of \sim 3.2 V. Considering both the cathode and anode materials, a higher energy density \sim 240 Wh kg⁻¹ is obtained. Rate capability and cycling performance of full cells were also tested, where a high capacity of \sim 280 mAh g⁻¹ could be remained even at a current rate of 1C, which is much better than that of half cells, and good cycling stability with ~95% capacity retention is observed after 50 cycles. The electrochemical performance of full cells suggests that this carbon anode shows the promising Na storage performance in NIBs.

In summary, a bi-honeycomb-like architecture of carbon anode material for NIBs has been synthesized by high-temperature treatment using a charcoal precursor at 1.900 °C. The resulting carbon materials show a mixed amorphous and graphitized components with the graphited carbon layer linking with large internal pores, which has not been reported in terms of hard carbon anodes. This carbon anode delivers a large proportion of the plateau capacity about 85% (>330 mAh g^{-1}) of its total reversible capacity (\sim 400 mAh g⁻¹) at the low potential below \sim 0.1 V. In addition, this carbon anode also shows the high initial Coulombic efficiency, good cycling performance and rate capability. The practical application of this carbon anode in full cells is further demonstrated by coupled with a layered Na_{0.9}Cu_{0.22}Fe_{0.30}Mn_{0.48}O₂ oxide cathode, the exhibited high-energy density of ${\sim}240\,Wh\,kg^{-1}$ is superior to the currently reported hard carbon anodes. This large-plateau capacity carbon anode is expected to further accelerate the commercialization of NIBs, and the further research remains to be explored, especially in the fundamental structure-function relationship between microstructure and electrochemical performance.

Conflict of interest

The authors declare that they have no conflict of interest.

Acknowledgments

This work was supported by the National Key Technologies R&D Program (2016YFB0901500) and National Natural Science Foundation of China (51725206, 51421002, 51232005, and 51372131).

References

- [1] Yang Z, Zhang J, Kintner-Meyer MCW, et al. Electrochemical energy storage for green grid. Chem Rev 2011;111:3577.
- [2] Zu CX, Li H. Thermodynamic analysis on energy densities of batteries. Energy Environ Sci 2011;4:2614.
- [3] Zhao C, Lu Y, Li Y, et al. Novel methods for sodium-ion battery materials. Small Methods 2017;1:1600063.
- [4] Palomares V. Casas-Cabanas M. Castillo-Martínez E. et al. Na-ion batteries. recent advances and present challenges to become low cost energy storage systems. Energy Environ Sci 2013;6:2312.
- [5] Pan H, Hu YS, Chen L. Room-temperature stationary sodium-ion batteries for large-scale electric energy storage. Energy Environ Sci 2013;6:2338.
 [6] Yabuuchi N, Kubota K, Dahbi M, et al. Research development on sodium-ion
- batteries. Chem Rev 2014;114:11636.
- [7] Zhao C, Wang Q, Lu Y, et al. Advanced Na metal anodes. J Phys D Appl Phys 2017:50:183001
- [8] Li Y. Lu Y. Zhao C. et al. Hard carbon microtubes made from renewable cotton as high-performance anode material for sodium-ion batteries. Energy Storage Mater 2017:7:130.
- [9] Mu L, Xu S, Li Y, et al. Prototype sodium-ion batteries using an air-stable and Co/Ni-free O3-layered metal oxide cathode. Adv Mater 2015;27:6928.
- [10] Li Y, Hu YS, Qi X, et al. Advanced sodium-ion batteries using superior low cost pyrolyzed anthracite anode: towards practical applications. Energy Storage Mater 2016:5:191.
- [11] Li Y, Mu L, Hu YS, et al. Pitch-derived amorphous carbon as high performance anode for sodium-ion batteries. Energy Storage Mater 2016;2:139.
- [12] Wang H, Liao XZ, Yang Y, et al. Large-scale synthesis of NaNi_{1/3}Fe_{1/3}Mn_{1/3}O₂ as high performance cathode materials for sodium ion batteries. I Electrochem Soc 2016:3:A565.
- [13] Bauer A, Song J, Vail S, et al. The scale-up and commercialization of nonaqueous Na-ion battery technologies. Adv Energy Mater 2018;8:1702869.
- [14] Wang Q, Zhao C, Lu Y, et al. Advanced nanostructured anode materials for sodium-ion batteries. Small 2017;13:1701835.
- [15] Yan G, Dugas R, Tarascon JM. The $Na_3V_2(PO_4)_2F_3/Carbon$ Na-ion battery: its performance understanding as deduced from differential voltage analysis. J Electrochem Soc 2018;165:A220.
- [16] Zhou Y, Yang Y, Jiao M, et al. What is the promising anode material for Na ion batteries? Sci Bull 2018;63:146.
- [17] Li Y, Xu S, Wu X, et al. Amorphous monodispersed hard carbon microspherules derived from biomass as a high performance negative electrode material for sodium-ion batteries. J Mater Chem A 2015;3:71.
- [18] Bommier C, Surta TW, Dolgos M, et al. New mechanistic insights on Na-ion storage in nongraphitizable carbon. Nano Lett 2015;15:5888.
- [19] Chen S, Ao Z, Sun B, et al. Porous carbon nanocages encapsulated with tin nanoparticles for high performance sodium-ion batteries. Energy Storage Mater 2016;5:180.
- [20] Li Z, Jian Z, Wang X, et al. Hard carbon anodes of sodium-ion batteries: undervalued rate capability. Chem Commun 2017;53:2610.
- Patra J, Huang HT, Xue W, et al. Moderately concentrated electrolyte improves solid-electrolyte interphase and sodium storage performance of hard carbon. Energy Storage Mater 2019;16:146.
- [22] Jin J, Yu BJ, Shi ZQ, et al. Lignin-based electrospun carbon nanofibrous webs as free-standing and binder-free electrodes for sodium ion batteries. J Power Sources 2014;272:800.

- [23] Gaddam RR, Yang DF, Narayan R, et al. Biomass derived carbon nanoparticle as anodes for high performance sodium and lithium ion batteries. Nano Energy 2016:26:346.
- [24] Li M, Feng N, Liu M, et al. Hierarchically porous carbon/red phosphorus composite for high-capacity sodium-ion battery anode. Sci Bull 2018:63:982-9.



Chenglong Zhao received his B.S and B.Admin. degrees from China University of Geosciences in Beijing in 2015. After that, he works as a postgraduate researcher following Prof. Yong-Sheng Hu in Institute of Physics, Chinese Academy of Sciences (IOP-CAS) on novel energy storage and conversion materials. His research interests focus on the preparation and characterization of inorganic crystal materials.



Yaxiang Lu is an associate professor at Institute of Physics of the Chinese Academy of Sciences (IOP-CAS). She received her Ph.D. degree from the University of Birmingham (UK) and moved to the University of Surrey (UK) to work as a research fellow. She was later awarded the "International Young Scientist Fellowship" by IOP-CAS and became an associate professor afterwards. Her research interests focus on advanced materials for energy storage and conversion, particularly on electrode materials for sodium-ion batteries recently.



Yong-Sheng Hu is a full professor at Institute of Physics, Chinese Academy of Sciences (IOP-CAS). He is working on advanced materials for long-life stationary batteries and their energy storage mechanisms, particularly focusing on sodium based batteries. He received several awards, such as The National Science Fund for Distinguished Young Scholars, The 14th China Youth Science and Technology Award, Tajima Prize, etc.